Available online at www.sciencedirect.com
ScienceDirect
Virus Research 127 (2007) 116–121
Virus Research
www.elsevier.com/locate/virusres

Short communication

Intracellular localization of the SARS coronavirus protein 9b: Evidence of active export from the nucleus

Igor Moshynskyy [a], Sathiyanarayanan Viswanathan [a], Natalia Vasilenko [a], Vladislav Lobanov [a], Martin Petric [b], Lorne A. Babiuk [a], Alexander N. Zakhartchouk [a,*]

[a] *Vaccine and Infectious Disease Organization (VIDO), University of Saskatchewan, 120 Veterinary Road, Saskatoon, SK S7N 5E3, Canada*
[b] *The University of British Columbia Centre for Disease Control, Vancouver, BC V5Z 4R4, Canada*

Received 5 January 2007; received in revised form 8 March 2007; accepted 14 March 2007
Available online 19 April 2007

Abstract

Open reading frame 9b (ORF 9b) encodes a 98 amino acid group-specific protein of severe acute respiratory syndrome (SARS) coronavirus (CoV). It has no homology with known proteins and its function in SARS CoV replication has not been determined. The N-terminal part of the 9b protein was used to raise polyclonal antibodies in rabbits, and these antibodies could detect 9b protein in infected cells. We analyzed the sub-cellular localization of recombinant 9b protein using fluorescence microscopy of live transfected cells and indirect immunofluorescence of transfected fixed cells. Our findings indicate that the 9b protein is exported outside of a cell nucleus and localizes to the endoplasmic reticulum. Our data also suggest that the 46-LRLGSQLSL-54 amino acid sequence of 9b functions as a nuclear export signal (NES).

Keywords: SARS coronavirus; Protein 9b; Nuclear export

Severe acute respiratory syndrome (SARS) first appeared in Guangdong Province, Southern China in November 2002. This newly emerging infectious disease quickly spread to 29 countries on five continents along international air travel routes, causing large-scale outbreaks in Hong Kong, Singapore and Toronto in early 2003.

A novel coronavirus was identified as the etiological agent of SARS (Peiris et al., 2003). The SARS coronavirus (CoV) is an enveloped virus with a positive single-stranded RNA genome of 29,727 nucleotides (Marra et al., 2003; Rota et al., 2003). The genome contains open reading frames (ORFs) which can encode the replicase, four main structural proteins, as well as proteins that vary in length from 39 to 274 amino acids with no homology to other coronaviruses. These proteins are often referred to as group-specific, because despite the absence of homology, they can be found in each of the four groups of coronaviruses while their sequence and their genes location differ among the groups.

Expression of group-specific proteins does not appear to be essential for CoV replication in cultured cells (Haijema et al., 2003). However, there are indications that strains in which these genes have been deleted may be attenuated in in vivo models of CoV infection (Ortego et al., 2003) and that expression of SARS CoV group-specific proteins by an attenuated murine CoV may substantially increase its virulence (Pewe et al., 2005). These observations suggest a possible role for these group-specific proteins in CoV pathogenesis. The objective of the present study was the characterization of the novel SARS-CoV group-specific protein 9b.

The SARS-CoV ORF 9b (also known as ORF13) overlaps with the nucleocapsid gene and encodes a 98-amino-acid protein. Antibodies against the 9b protein were found in the sera of convalescent patients (Guo et al., 2004; Qiu et al., 2005; Zhong et al., 2005), and expression of this protein was demonstrated in diseased organs and SARS-CoV infected cells by immunohistochemistry (Chan et al., 2005). Recently, the crystal structure of 9b has been resolved (Meier et al., 2006). The protein has a novel fold, a dimeric tent-like beta structure with an amphipathic surface, and a central hydrophobic cavity that binds lipid molecules.

In our study, the ORF 9b gene was amplified from RNA of SARS-CoV-infected Vero E6 cells (strain Tor 2) using a one step RT PCR kit (Qiagen) (see Table 1 for primer sequences)

* Corresponding author. Tel.: +1 306 966 1570; fax: +1 306 966 7478.
E-mail address: alex.zak@usask.ca (A.N. Zakhartchouk).

0168-1702/$ – see front matter © 2007 Elsevier B.V. All rights reserved.
doi:10.1016/j.virusres.2007.03.011

Table 1
Primers used in this study

Primer	Sequence[a]	Sense	Application
ORF13FOR	CG**GGATCC**ATGGACCCCAATCAAACCAA	+	pcDNA-9b
ORF13STOP	G**GAATTC**TCATTTTGCCGTCACCACCACGA	−	pcDNA-9b
ORF13GEXF	G**GAATTC**TGATGGACCCCAATCAAACCAA	+	pGEX-9bN and p9b-EYFP
ORF13XHO	GGTCATCTGGACCACTATTG	−	pGEX-9bN
13REVBCL	T**TGATCA**TTTGCCGTCACCACCACGAACG	−	p9b-EYFP

[a] Restriction sites introduced into primers are in bold.

and cloned into a pcDNA3 (Invitrogen) vector into *Bam*HI and *Eco*RI sites to create pcDNA-9b. Next, a 196-bp fragment of the gene was amplified by PCR (primers are listed in the Table 1), digested with *Eco*RI and *Xho*I and subcloned in frame with the glutathione-*S*-transferase (GST) gene in *Eco*RI and *Xho*I sites of the vector pGEX5X2 (Amersham Biosciences) to create pGEX-9bN. Expression of the recombinant GST-9b fusion protein in bacteria was induced in the presence of 0.1 mM isopropyl beta-D-thiogalactopyranoside. Proteins from the induced bacterial cultures were separated by SDS-polyacrylamide gel electrophoresis and the GST-9b fusion protein was eluted from the gel by the "crush and soak" method (Sambrook et al., 1989). This gel-purified protein was used to immunize New Zealand White rabbits in order to generate anti-9b serum. The generated rabbit polyclonal antibodies were used for detection of expression of ORF 9b gene in cultured cells infected with SARS CoV. Near-confluent monolayer of cultured Vero E6 cells was inoculated with SARS-CoV at a multiplicity of infection (MOI) of 0.1 plaque forming units per cell. Forty-eight hours post infection the cells were harvested and lysed in 1% SDS.

The expression of the 9b protein in African green monkey kidney cells of Vero E6 lineage (derivative of the ATCC line CCL-81) was demonstrated by Western blot analysis. Total proteins from infected cells were separated by 15% polyacrylamide SDS gel electrophoresis in Tris–Tricine buffer, immobilized on a nitrocellulose membrane and probed with polyclonal rabbit serum raised as described above against recombinant 9b protein (Fig. 1). A unique protein band was detected in the extracts from infected Vero E6 cells (Fig. 1, Panel B, lane 1) while such a band was not present in protein extracts from non-infected cells (Panel B, lane 2), which indicated that ORF 9b was expressed during SARS-CoV infection and could be detected by specific rabbit polyclonal antibodies. Using these antibodies, the protein of a similar electrophoretic mobility was detected in HEK 293 cells infected with recombinant adenovirus expressing the 9b protein (Fig. 1, Panel A, lane 1). Adenovirus expressing the 9b protein was constructed using AdenoEasy Ad5 homologous recombination kit (CLONTECH). The observed electrophoretic mobility of the protein extracted from the infected cells was between 10 and 15 kDa which is close to the 11 kDa calculated molecular weight of the 9b protein. To our knowledge, this is the first Western blot analysis of the 9b protein.

Since biological processes are directed and regulated in different cellular compartments, it is commonly agreed that obligatory intracellular parasites such as viruses would depend on appropriate trafficking of host and viral molecules important for completion of the viral replication cycle and respective metabolic pathways. It would be interesting to study the subcellular localization of the 9b protein in the SARS-CoV-infected cells using anti-9b antibodies for immunofluorescence. Unfortunately, anti-9b rabbit serum we developed in this study appeared to show a background cross-reactivity with proteins in uninfected cultured cells (data not shown), which made it unsuitable for conclusive demonstration of the cellular localization of the 9b in the SARS-CoV infected cells. Therefore, we examined cellular localization of recombinant 9b tagged with enhanced

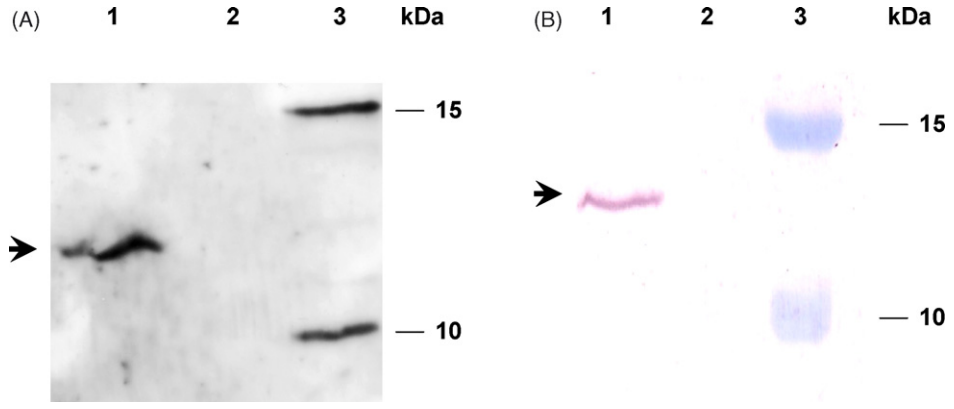

Fig. 1. Immunoblot of total cellular proteins of cells expressing 9b and probed with anti-9b rabbit serum. (A) Expression of 9b by 293 HEK cells infected with adenovirus encoding 9b; lane 1, total protein extract from 293 HEK cells infected with recombinant adenovirus encoding 9b; lane 2, total protein extract from uninfected 293 HEK cells; lane 3, Precision Plus Protein Standard (BioRad). (B) Expression of the 9b by Vero E6 cells infected with SARS coronavirus. Lane 1, total protein extract from Vero E6 cells infected with SARS-CoV; lane 2, total protein extract from uninfected Vero E6 cells; lane 3, PageRuler Prestained Protein Ladder Plus (Fermentas). Size of the protein standards indicated on the right. Arrow indicates the position of the unique 9b-specific protein band.

yellow-green variant of the *Aequorea victoria* green fluorescent protein (EYFP) protein or with FLAG epitope by fluorescence microscopy in transfected Vero E6 cells.

To construct a plasmid encoding the in-frame fusion of 9b to the N-terminus of EYFP, the gene for 9b was PCR amplified (see Table 1 for primer sequences), cut with *Eco*RI and *Bcl*I and cloned into pEYFP-N1 (CLONTECH) vector digested with *Eco*RI and *Bam*HI to create p9b-EYFP. The construct was analyzed by restriction endonuclease digest (data not shown) and the in-frame fusion was confirmed by DNA sequencing.

Vero E6 cells were transiently transfected with p9b-EYFP using a calcium phosphate transfection kit (Promega). Vero E6 cells transfected with the pEYFP-N1 encoding an unmodified EYFP were used as controls for the intracellular distribution of EYFP green fluorescence without 9b. Forty eight hours post transfection, the cellular distribution of the green fluorescence was examined using a ZEISS model Axiovert 200M microscope and photographed (Fig. 2a and d) using a 520 nm filter. Cell nuclei were counter-stained with Hoechst 33342 (Sigma) (Fig. 2b and e) and the images of the same view fields were taken using a 370 nm filter. Comparison of the images and intensity of green fluorescence indicated that the 9b-EYFP fusion protein was distributed predominantly in the cytoplasm with the highest fluorescence intensity being observed in a perinuclear space, while the amount of the fusion protein in the nuclei of Vero E6 cells was substantially reduced (Fig. 2d–g). In contrast, unmodified EYFP was distributed evenly throughout the cell, with slightly higher fluorescence in the nucleus of transfected Vero E6 cells (Fig. 2a–c). This suggests that 9b was responsible for the observed intracellular distribution of 9b-EYFP fusion protein.

Since the endoplasmic reticulum/Golgi intermediate compartment (ERGIC) is believed to be the primary site for coronavirus assembly and budding (Garoff et al., 1998), colocalization with the Golgi complex may indicate a possible role of a viral protein in either budding or virion assembly. In order to determine the location of the Golgi apparatus, live transfected Vero E6 cells were stained with C5 ceramides (BODIPY TR ceramide, Invitrogen) followed by photographing of the same view fields using a 600 nm filter (Fig. 2f). Images of the same view field were superimposed (Fig. 2g) using Adobe Photoshop CS2 software (Adobe Systems Inc.) and the intracellular distribution of green fluorescence was examined. It was determined that green fluorescence of the 9b-EYFP only partially overlapped with red fluorescence of the Golgi complex (Fig. 2g), suggesting that 9b was not targeted exclusively to Golgi.

In order to eliminate the possibility that either conformational changes in the fusion construct or a novel amino acid sequence formed at the point of fusion, affected intracellular distribution of the fluorescent fusion protein, 9b was tagged with the FLAG epitope. The gene for 9b was cut out from pcDNA-9b with *Hin*dIII and *Eco*RI and cloned into *Hin*dIII and *Eco*RI sites of pFLAG-CMV2 (Sigma) to create pFLAG-9b. The sequence of the resulting plasmid was confirmed by restriction endonuclease analysis and DNA sequencing (data not shown).

Vero E6 cells cultured on slides were transfected with pFLAG-9b as above, fixed in ice-cold methanol for 10 min and probed with murine monoclonal anti-FLAG antibodies (Sigma). To visualize an intracellular distribution of FLAG-9b fusion protein, slides were treated with FITC-conjugated goat anti-mouse secondary antibodies (BD Biosciences) and examined by fluorescence microscopy (Fig. 2h). Nuclear counterstaining was done as above (Fig. 2i). Additionally, the cells were stained with ERtracker™ Red Dye (Invitrogen) (selective for endoplasmic reticulum), which was visualized using TRITC (600 nm) filter (Fig. 2j). Superimposition of fluorescence images (Fig. 2k) was performed as outlined above.

Analysis of the fluorescence images indicated that the FLAG-9b fusion protein was distributed predominantly outside of the cell nuclei, with the highest fluorescence signal intensity found in the perinuclear space (Fig. 2h–k). This was consistent with the results obtained with 9b-EYFP fusion protein and suggested that 9b was associated with the extranuclear localization of both fusion proteins. Staining of transfected fixed cells with ERtracker indicated that FLAG-9b fusion protein was localized to the endoplasmic reticulum (Fig. 2k).

To further verify localization of the 9b protein to the endoplasmic reticulum, Vero E6 cells transfected with the 9b-EYFP construct were fixed as above, stained with ERtracker and analyzed using a Zeiss LSM410 confocal microscope equipped with external Argon Ion Laser. Enhanced yellow fluorescence protein was excited by Argon Ion Laser beam (488 nm), while ERtracker was excited by Helium/Neon Laser beam (594 nm). Both signals were detected simultaneously, separate images were taken and superimposed as described above (Fig. 2l–n). Confocal images further confirmed localization of 9b to the endoplasmic reticulum (Fig. 2n).

Interestingly, a confocal microscopy of the 9b-EYFP transfected cells and an indirect immunofluorescence staining of transfected Vero E6 cells with anti-FLAG antibodies revealed cytoplasmic inclusion bodies of 9b protein, whereas live cells transfected with p9b-EYFP showed diffuse cytoplasmic fluorescence. These differences may be explained by cell fixation or by influence of the tags on 9b distribution patterns. Moreover, Meier et al. (2006) have recently shown speckled cytoplasmic localization of the 9b in transfected 293T cells, which were fixed and stained with an anti-His tag fluorochrome-conjugated monoclonal antibody.

Since the diameter of a nuclear pore (Paine et al., 1975) allows passive passage of ions and small proteins (less than 60 kDa) (van der Aa et al., 2006), it can be presumed that either unmodified 9b (11 kDa), EYFP (27 kDa), or 9b-EYFP fusion protein (38 kDa), may be capable of passive diffusion between the nucleus and the cytoplasm. This assumption was consistent with the observed subcellular distribution of an unmodified EYFP (Fig. 2a) which was homogenously distributed both in the nuclei and the cytoplasm. In contrast, 9b-EYFP fusion was excluded from the nucleus (Fig. 2d), and such exclusion could be explained by active extranuclear transport.

The amino acid sequence of the 9b protein (Accession number AAP41048) was analyzed using publicly available protein sequence analysis tools (la Cour et al., 2003) at http://www.cbs.dtu.dk. Amino acid residues 46-LRLGSQLSL-54 were predicted to form a nuclear export sequence (NES).

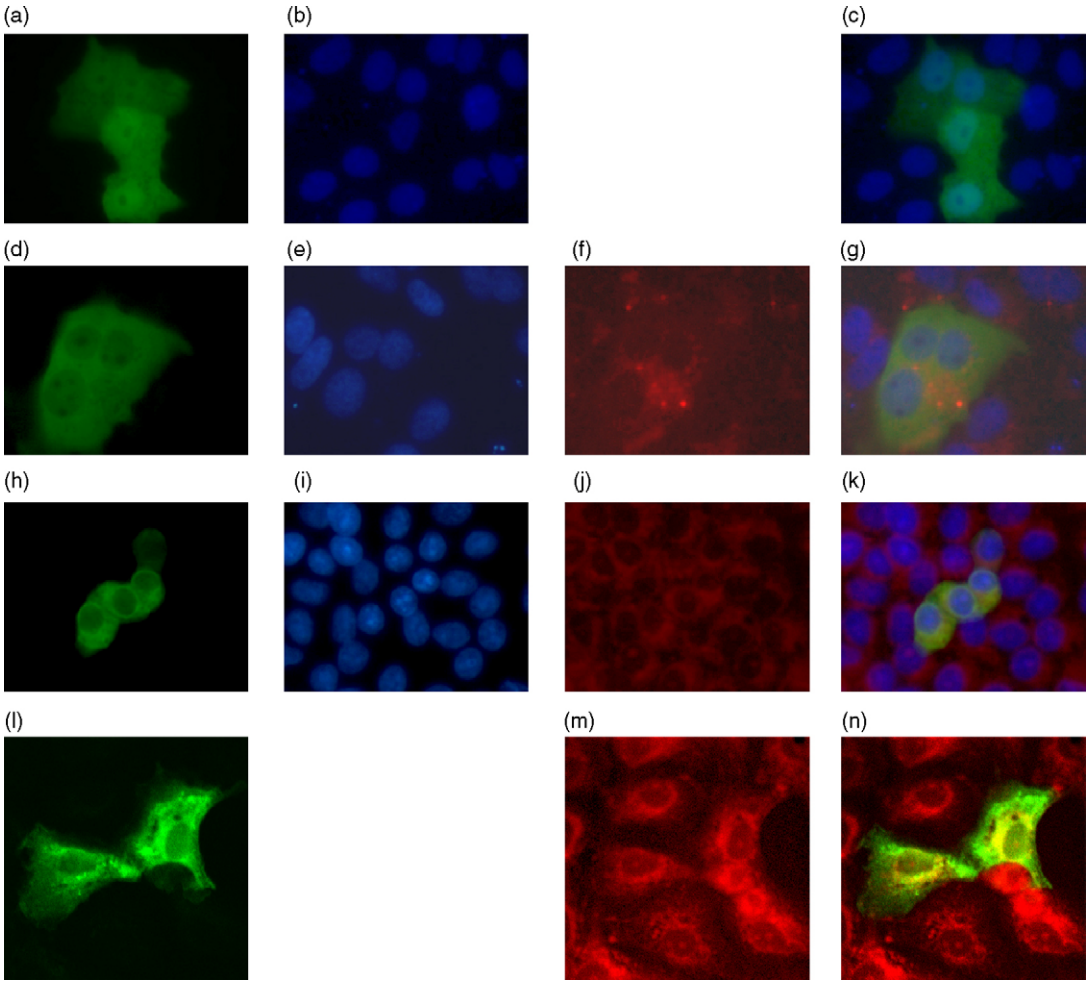

Fig. 2. Subcellular localization of recombinant 9b protein in transiently transfected Vero E6 cells. *Top row*: Vero E6 cells transfected with the plasmid expressing EYFP: (a) fluorescence of cells expressing EYFP; (b) nuclei stained with Hoechst 33342; (c) merge of images a and b. *Second row*: Vero E6 cells transfected with the plasmid expressing 9b-EYFP fusion protein: (d) fluorescence in the cells expressing 9b-EYFP protein; (e) nuclei stained with Hoechst 33342; (f) Golgi complex stained with C5 ceramide BODIPY TR; (g) merge of images d, e and f. *Third row*: indirect immunofluorescence of Vero E6 cells transfected with the plasmid expressing the FLAG-9b fusion protein: (h) fixed cells probed with monoclonal murine anti-FLAG antibodies and visualized with Goat anti-mouse FITC-conjugated serum; (i), nuclei stained with Hoechst 33342; (j) endoplasmic reticulum stained with ERtracker™ Red; (k) merge of images h, i and j. *Bottom row*: confocal fluorescence microscopy of Vero E6 cells transfected with 9b-EYFP: (l) green fluorescence of the fusion protein; (m) endoplasmic reticulum stained with ERtracker™ Red; (n) merge of images l and m.

This amino acid sequence represents a novel NES, belonging to the $LX_{1–3}LX_{2–4}LXL$ protein motif, where X is any amino acid (Rodriguez et al., 2003; Wen et al., 1995). This motif acting as a nuclear export signal has been found in a series of proteins including mitogen-activated protein kinase kinase (MAPKK) (Fukuda et al., 1996), Rev protein of the human immunodeficiency virus (Fukuda et al., 1997) and an inhibitor of cAMP-dependent protein kinase (PKI) (Wen et al., 1994). Nucleocytoplasmic proteins with leucine-rich NES sequences are transported across the nuclear envelope through nuclear pores out of the cell nucleus by an energy-dependent mechanism using exportin 1 (Ossareh-Nazari et al., 1997; Fornerod et al., 1997).

To prove that 46-LRLGSQLSL-54 may function as a NES, we used two approaches. First, we investigated the effect of leptomycin B on the cytoplasmic localization of 9b in transfected Vero E6 cells. Leptomycin B inhibits NES-dependent export of NES-containing proteins (Wolff et al., 1997) by binding to exportin 1 and preventing assembly of the NES-exportin 1 complexes (Ossareh-Nazari et al., 1997). Second, we generated a mutant 9b in which codons for leuicine residues L46, L48, L52 and L54 were replaced by codons for glycine. In order to generate this mutant, a synthesis of the 297 bp ORF 9b gene with mutated codons was ordered from EZBiolab Inc. (Wesfield, IN, USA), and the gene was cloned into the pEYFP-N1 vector in frame with the EYFP gene creating the plasmid p9bDeltaNES-EYFP.

When Vero E6 cells transiently transfected with the ORF 9b-EYFP fusion construct were incubated in growth medium containing 20 nM leptomycin B (Sigma) for 24 h, the intracellular distribution of green fluorescence (Fig. 3a–c) differed from that of untreated cells transfected with ORF 9b-EYFP fusion construct (Fig. 2d). Essentially, it was similar to the distribution of the green fluorescence in cells transfected with the pEYFP-N1 vector (Fig. 2a).

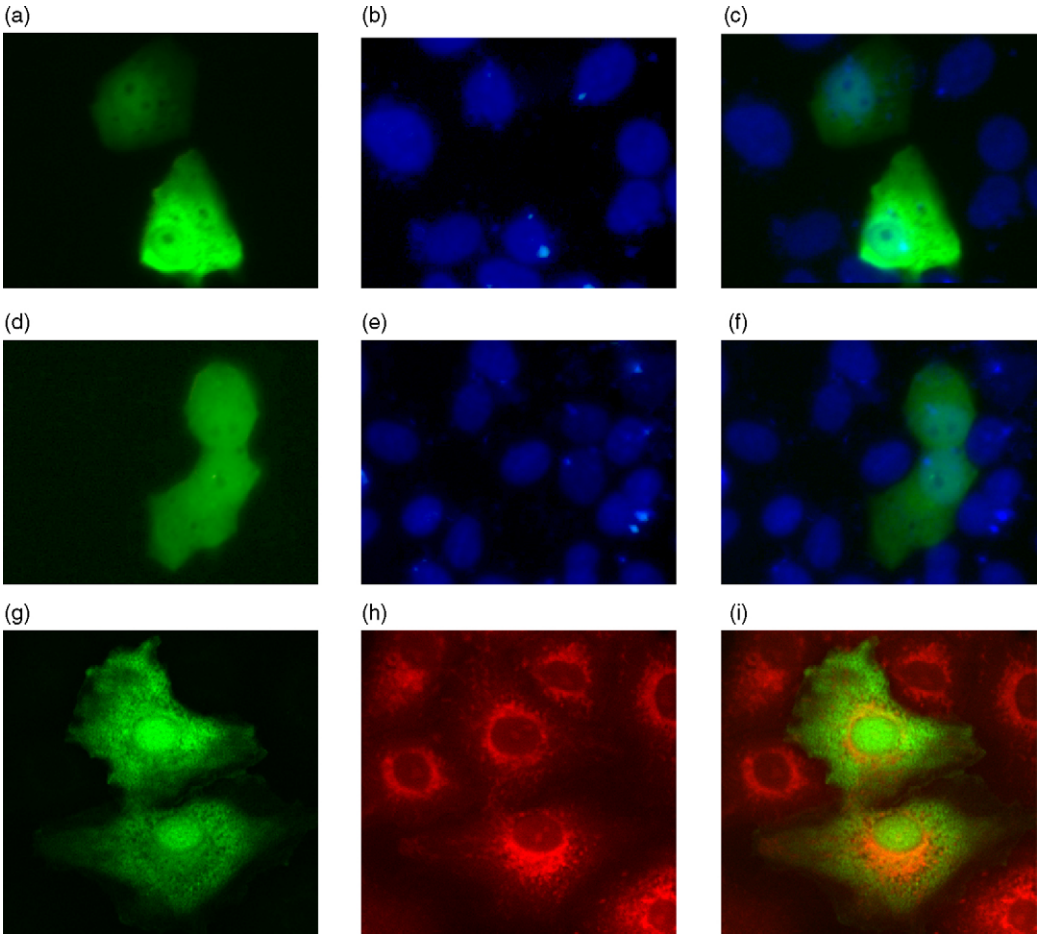

Fig. 3. Role of a nuclear export sequence (NES) in subcellular localization of recombinant 9b in transiently transfected Vero E6 cells. *Top*: (a) fluorescence in Vero E6 cells expressing 9b-EYFP fusion protein after 24 h treatment with leptomycin B; (b) nuclei stained with Hoechst 33342; (c) merge of images a and b. *Middle*: (d) fluorescence in Vero E6 cells expressing 9bDeltaNES-EYFP fusion protein; (e) nuclei stained with Hoechst 33342; (f) merge of images d and e. *Bottom*: confocal microscopy of Vero E6 cells expressing 9bDeltaNES-EYFP fusion protein: (g) green fluorescence of the 9bDeltaNES-EYFP fusion protein; (h) endoplasmic reticulum stained with ERtracker^{TM} Red; (i) merge of images g and h.

Similarly, the character of distribution of the green fluorescence in cells transfected with p9bDeltaNES-EYFP (Fig. 3d–f), repeated that of the cells transfected with pEYFP (Fig. 2a). In addition, confocal microscopy of Vero E6 cells transfected with p9bDeltaNES-EYFP (Fig. 3g–i) indicated that the alteration of the NES of the 9b aborted predominantly extranuclear localization of green fluorescence. Taken together, these data suggest that cytoplasmic localization of 9b results from its transport from the nucleus to the cytoplasm by interaction with exportin 1 via a leucine-rich NES.

Acknowledgements

We want to thank Mr. Barry Carroll for immunization of rabbits. We thank Saskatchewan Structural Sciences Centre (University of Saskatchewan, Saskatoon) for help in confocal microscopy. This work was supported by Canadian Institute for Health Research grant and Saskatchewan Health Research Foundation (fellowship for Dr. Moshynskyy). Published as VIDO Journal article # 448.

References

Chan, W.S., Wu, C., Chow, S.C., Cheung, T., To, K.F., Leung, W.K., Chan, P.K., Lee, K.C., Ng, H.K., Au, D.M., Lo, A.W., 2005. Coronaviral hypothetical and structural proteins were found in the intestinal surface enterocytes and pneumocytes of severe acute respiratory syndrome (SARS). Modern Pathol. 18, 1432–1439.

Fornerod, M., Ohno, M., Yoshida, M., Mattaj, I.W., 1997. CRM1 is an export receptor for leucine-rich nuclear export signals. Cell 90, 1051–1060.

Fukuda, M., Asano, S., Nakamura, T., Adachi, M., Yoshida, M., Yanagida, M., Nishida, E., 1997. CRM1 is responsible for intracellular transport mediated by the nuclear export signal. Nature 390, 308–311.

Fukuda, M., Gotoh, I., Gotoh, Y., Nishida, E., 1996. Cytoplasmic localization of mitogen-activated protein kinase kinase directed by its NH_2-terminal, leucine-rich short amino acid sequence, which acts as a nuclear export signal. J. Biol. Chem. 271, 20024–20028.

Garoff, H., Hewson, R., Opstelten, D.J., 1998. Virus maturation by budding. Microbiol. Mol. Biol. Rev. 62, 1171–1190.

Guo, J.P., Petric, M., Campbell, W., McGeer, P.L., 2004. SARS corona virus peptides recognized by antibodies in the sera of convalescent cases. Virology 32, 251–256.

Haijema, B.J., Volders, H., Rottier, P.J., 2003. Switching species tropism: an effective way to manipulate the feline coronavirus genome. J. Virol. 77, 4528–4538.

la Cour, T., Gupta, R., Rapacki, K., Skriver, K., Poulsen, F.M., Brunak, S., 2003. NESbase version 1.0: a database of nuclear export signals. Nucleic Acids Res. 31, 393–396.

Marra, M.A., Jones, S.J., Astell, C.R., Holt, R.A., Brooks-Wilson, A., Butterfield, Y.S., Khattra, J., Asano, J.K., Barber, S.A., Chan, S.Y., Cloutier, A., Coughlin, S.M., Freeman, D., Girn, N., Griffith, O.L., Leach, S.R., Mayo, M., McDonald, H., Montgomery, S.B., Pandoh, P.K., Petrescu, A.S., Robertson, A.G., Schein, J.E., Siddiqui, A., Smailus, D.E., Stott, J.M., Yang, G.S., Plummer, F., Andonov, A., Artsob, H., Bastien, N., Bernard, K., Booth, T.F., Bowness, D., Czub, M., Drebot, M., Fernando, L., Flick, R., Garbutt, M., Gray, M., Grolla, A., Jones, S., Feldmann, H., Meyers, A., Kabani, A., Li, Y., Normand, S., Stroher, U., Tipples, G.A., Tyler, S., Vogrig, R., Ward, D., Watson, B., Brunham, R.C., Krajden, M., Petric, M., Skowronski, D.M., Upton, C., Roper, R.L., 2003. The genome sequence of the SARS-associated coronavirus. Science 300, 1399–1404.

Meier, C., Aricescu, A.R., Assenberg, R., Aplin, R.T., Gilbert, R.J.C., Grimes, J.M., Stuart, D.I., 2006. The crystal structure of ORF-9b, a lipid binding protein from the SARS coronavirus. Structure 14, 1157–1165.

Ortego, J., Sola, I., Almazan, F., Ceriani, J.E., Riquelme, C., Balasch, M., Plana, J., Enjuanes, L., 2003. Transmissible gastroenteritis coronavirus gene 7 is not essential but influences in vivo virus replication and virulence. Virology 308, 13–22.

Ossareh-Nazari, B., Bachelerie, F., Dargemont, C., 1997. Evidence for a role of CRM1 in signal-mediated nuclear protein export. Science 278, 141–144.

Paine, P.L., Moore, L.C., Horowitz, S.B., 1975. Nuclear envelope permeability. Nature 254, 109–114.

Peiris, J.S., Yuen, K.Y., Osterhaus, A.D., Stohr, K., 2003. The severe acute respiratory syndrome. N. Engl. J. Med. 349, 2431–2441.

Pewe, L., Zhou, H., Netland, J., Tangudu, C., Olivares, H., Shi, L., Look, D., Gallagher, T., Perlman, S., 2005. A severe acute respiratory syndrome-associated coronavirus-specific protein enhances virulence of an attenuated murine coronavirus. J. Virol. 79, 11335–11342.

Qiu, M., Shi, Y., Guo, Z., Chen, Z., He, R., Chen, R., Zhou, D., Dai, E., Wang, X., Si, B., Song, Y., Li, J., Yang, L., Wang, J., Wang, H., Pang, X., Zhai, J., Du, Z., Liu, Y., Zhang, Y., Li, L., Wang, J., Sun, B., Yang, R., 2005. Antibody responses to individual proteins of SARS coronavirus and their neutralization activities. Microbes. Infect. 7, 882–889.

Rodriguez, J.A., Span, S.W., Kruyt, F.A., Giaccone, G., 2003. Subcellular localization of CrmA: identification of a novel leucine-rich nuclear export signal conserved in anti-apoptotic serpins. Biochem. J. 373, 251–259.

Rota, P.A., Oberste, M.S., Monroe, S.S., Nix, W.A., Campagnoli, R., Icenogle, J.P., Penaranda, S., Bankamp, B., Maher, K., Chen, M.H., Tong, S., Tamin, A., Lowe, L., Frace, M., DeRisi, J.L., Chen, Q., Wang, D., Erdman, D.D., Peret, T.C., Burns, C., Ksiazek, T.G., Rollin, P.E., Sanchez, A., Liffick, S., Holloway, B., Limor, J., McCaustland, K., Olsen-Rasmussen, M., Fouchier, R., Gunther, S., Osterhaus, A.D., Drosten, C., Pallansch, M.A., Anderson, L.J., Bellini, W.J., 2003. Characterization of a novel coronavirus associated with severe acute respiratory syndrome. Science 300, 1394–1399.

Sambrook, J., Fritsch, E.F., Maniatis, T., 1989. Molecular Cloning: A Laboratory Manual, second ed. Cold Spring Harbor Laboratory Press, New York.

van der Aa, M.A., Mastrobattista, E., Oosting, R.S., Hennink, W.E., Koning, G.A., Crommelin, D.J., 2006. The nuclear pore complex: the gateway to successful nonviral gene delivery. Pharm. Res. 23, 447–459.

Wen, W., Harootunian, A.T., Adams, S.R., Feramisco, J., Tsien, R.Y., Meinkoth, J.L., Taylor, S.S., 1994. Heat-stable inhibitors of cAMP-dependent protein kinase carry a nuclear export signal. J. Biol. Chem. 269, 32214–32220.

Wen, W., Meinkoth, J.L., Tsien, R.Y., Taylor, S.S., 1995. Identification of a signal for rapid export of proteins from the nucleus. Cell 82, 463–473.

Wolff, B., Sanglier, J.J., Wang, Y., 1997. Leptomycin B is an inhibitor of nuclear export: inhibition of nucleo-cytoplasmic translocation of the human immunodeficiency virus type 1 (HIV-1) Rev protein and Rev-dependent mRNA. Chem. Biol. 4, 139–147.

Zhong, X., Yang, H., Guo, Z.F., Sin, W.Y., Chen, W., Xu, J., Fu, L., Wu, J., Mak, C.K., Cheng, C.S., Yang, Y., Cao, S., Wong, T.Y., Lai, S.T., Xie, Y., Guo, Z., 2005. B-cell responses in patients who have recovered from severe acute respiratory syndrome target a dominant site in the S2 domain of the surface spike glycoprotein. J. Virol. 79, 3401–3408.